ARE MUSCLE FIBERS WITHIN FISH MYOTOMES ACTIVATED SYNCHRONOUSLY? PATTERNS OF RECRUITMENT WITHIN DEEP MYOMERIC MUSCULATURE DURING SWIMMING IN LARGEMOUTH BASS

BRUCE C. JAYNE[1] AND GEORGE V. LAUDER[2]

[1]*Department of Biological Sciences, University of Cincinnati, Cincinnati, OH 45221-0006, USA* and
[2]*Department of Ecology and Evolutionary Biology, University of California, Irvine, CA 92717, USA*

Summary

The myomeric axial musculature of fish has a complex three-dimensional morphology, yet within-myomere motor patterns have not been examined to determine whether all portions of each myomere are activated synchronously during locomotion. To gain insight into recruitment patterns in the deep myomeric musculature of fish, we implanted a series of fine-wire electrodes arranged in a vertical row of six electrodes and a longitudinal row of three electrodes on both the left and right sides of each of five largemouth bass (*Micropterus salmoides*). After recording electromyograms (EMGs) during the burst-and-glide swimming of each fish, *post-mortem* dissections and X-rays determined the location of electrodes with respect to (1) the longitudinal position (by counting the underlying vertebrae), (2) the position of the myomere containing the electrode, and (3) the portion within each myomere containing an electrode. Because of the convoluted overlapping shape of the myomeres, electrodes within the vertical row of sites could be located in any one of six different myomeres. Thus, we compared muscle activity for locations with a constant longitudinal position and differing myomeric position (vertical row) and among sites with both variable longitudinal and myomeric positions. We detected significant heterogeneity in EMG onset times for sites within the vertical row of electrodes; however, the durations of the EMGs from different sites were similar. EMG onset times at more posterior longitudinal positions preceded those of more anterior longitudinal positions when electrodes of the latter site were within a more posterior myomere. Thus, the timing of EMGs was consistent with the posterior propagation of muscle activity *via* the sequential activation of myomeres rather than the simultaneous activation of all contractile tissue within the longitudinal span of a single vertebra. In addition, extreme epaxial and hypaxial portions of myomeres showed distinct activity patterns which did not necessarily correlate with activity in the central myomeric fibers nearer the horizontal septum.

Key words: muscle, electromyography, locomotion, swimming, fish, *Micropterus salmoides*.

Introduction

To a variable extent within different lineages of chordates, axial structures display a segmented organization. The segmented arrangement of the vertebrate axial skeleton is especially familiar since it is apparent in both fossil remains and in extant taxa. However, the presence of segmented axial musculature in non-vertebrate chordates, such as *Branchiostoma* and the hagfish (Bone, 1989), suggests that the myomeric organization of axial muscle may actually have preceded the evolution of a segmented axial skeleton among vertebrate ancestors. Among extant vertebrate taxa, the myomeric arrangement of the axial muscles in fish is a classic example of segmented (metameric) organization. Although there are equal numbers of muscular and skeletal segments in fish, several vertebrae are spanned by the contractile tissue of a single myomere as a result of its complex, convoluted shape

(Greene and Greene, 1914; Nursall, 1956; Westneat *et al.* 1993; Jayne and Lauder, 1994*a*).

The complicated shape and fiber orientation of myotomes has posed a challenge to understanding myomeric muscle function, and several authors have addressed this important issue from a morphological perspective in order to gain a better understanding of the undulatory axial locomotion of fish. For example, Alexander (1969) suggested that the fibers within a single myomere were arranged such that the combined contractile tissue of several different myomeres would collectively form a helical trajectory. Despite different orientations of the fibers from many different portions of myomeres at a given longitudinal location, Rome and Sosnicki (1991) found that the sarcomere lengths of the myomeric musculature were effectively identical for a given amount of

lateral bending. Thus, if all the myomeric muscle in a given cross section of the fish were activated simultaneously, these fibers would be operating at similar rates of strain and force production. Wainwright (1983) has emphasized that the connective tissue in both the myosepta and the skin of many fish is effective for resisting tensile loads, but is ineffective for resisting compressive forces. Consequently, the connective tissue could potentially constrain shape changes in active muscle resulting in the production of pressure that could be instrumental in flexing a fish laterally (Wainwright, 1983). Westneat *et al.* (1993) recently suggested that the activation of the deep portions of the myomere may be a mechanism for maintaining the orientation of tendons that is required for efficient transmission of forces developed by the superficial red fibers of scombrid fish. Critical information for all of these suggestions of myomeric function is the *in vivo* pattern of activity for the deep myomeric musculature, and we lack these important data.

Although some aspects of the innervation of the axial musculature of fish have been described, we also lack sufficient detail to make precise predictions for expected patterns of activation of the myomeric musculature. The deep myomeric muscle is innervated by large (primary) motoneurons which do not innervate the superficial red muscle that is near the horizontal septum (Fetcho, 1986). In zebrafish, three distinct primary motoneurons innervate different portions (territories) of each myomere and their axonal branches are confined to a single myomere. The territories of individual smaller (secondary) motoneurons may include fibers from more than one myomere as well as having some overlap with the territories of certain primary motoneurons (Westerfield *et al.* 1986). Individual muscle fibers within the myomeres commonly have polyneuronal distributed innervation (at least in percomorph teleost fish; Bone, 1989; Bone and Ono, 1982), but the number of motoneurons per fiber varies widely among different species of fish (Bone, 1978). In certain species, single muscle fibers may receive inputs from different spinal segments (Hudson, 1969), but the total number of spinal segments that send inputs to an entire myomere is not well documented for any species of fish. In light of the large numbers of motoneurons that are associated with a single myomere, many different motor patterns are theoretically possible for activation of myomeric muscle.

In this study, we used electromyography to determine *in vivo* patterns of recruitment within the deep myomeric musculature of the largemouth bass *Micropterus salmoides*. We used a pattern of electrode placement specifically designed to discriminate between two possible mutually exclusive patterns of muscle activity. One (of many) hypothetically possible pattern of muscle activity is that all of the contractile tissue in a myomere is activated synchronously. For locomotor behavior involving posteriorly propagated muscle activity, synchronous activation within a myomere would cause significant differences in the timing of muscle activity at a single longitudinal location because of the extensive longitudinal overlap of many different myomeres.

An alternative possibility is that all of the contractile tissue at a single longitudinal location is activated synchronously, and this would result in significant differences in the times of muscle activity within a single myomere, since these structures span several vertebrae. We implanted a large number of electrodes both within a single longitudinal position and at different longitudinal locations; hence, comparisons of the timing of muscle activity among different electrodes provide an experimental test of these alternative patterns of myomeric activity.

## Materials and methods
Experimental subjects and protocol

We obtained all specimens of *Micropterus salmoides* Lacepede largemouth bass) from ponds in southern and central California. The bass were fed a maintenance diet of earthworms and goldfish, and their times in captivity before experiments ranged from 3 to 6 months. All fish were maintained individually in 80 l tanks at a temperature of $20\pm2\,^{\circ}\mathrm{C}$, which averaged the same value as the water temperature that was used during experiments ($20\pm0.5\,^{\circ}\mathrm{C}$).

Preliminary experiments with six individuals were used to determine a suitable pattern of electrode placement and the swimming speeds at which the myomeric fibers were recruited. After standardizing the methodology, we performed and analyzed results from experiments that used five additional fish with mean values (and ranges) of mass, standard length (SL) and total length (TL) of 160 g (140–189 g), 20.8 cm (19.4–23.5 cm) and 23.3 cm (19.5–25.0 cm), respectively.

After electrodes had been implanted, fish were placed in a flow tank and allowed to recover from anesthesia for 2–3 h. The working section of the calibrated flow tank was 30 cm×30 cm in cross section with a length of 90 cm. Deep white muscle was generally not recruited until most fish used the burst-and-glide mode of unsteady swimming. For time intervals approximating 20–30 s, we used flow speeds ranging from 50 to 75 cm s^{-1} to elicit burst-and-glide swimming, with 65 cm s^{-1} being a particularly effective speed for eliciting the desired pattern of behavior. Two to three such periods of high flow speed were commonly interspersed with slower flow rates (approximately 25 cm s^{-1}) for a total of about 2–3 min of continuous videotaping. Between each 2–3 min session, the fish were allowed to rest for periods of 30 min to 2 h, until we finally obtained enough observations of suitable quality. One should note that, after a single kick, fish commonly advanced several centimeters upstream. Consequently, flow speeds underestimate swimming speeds but they do give an approximation of the speed of swimming just prior to the kick behavior.

Videotapes (synchronized with electromyographic recordings) were obtained of both lateral and ventral views simultaneously of the swimming fish using a NAC HSV-400 high-speed video system operating at 200 images s^{-1}. Videotapes were used primarily to discard data from sequences when the fish or the electrode cable contacted any of the walls

Fig. 1. Left lateral view (anterior is to the left) of complete myomere dissections in the region of *Micropterus salmoides* used for electromyographic experiments. Most anteriorly, four myomeres have been completely removed, and three complete myomeres have been removed on either side of the more posterior intact myomere. The total length of this individual was 25.2 cm. Scale bar, 1 cm.
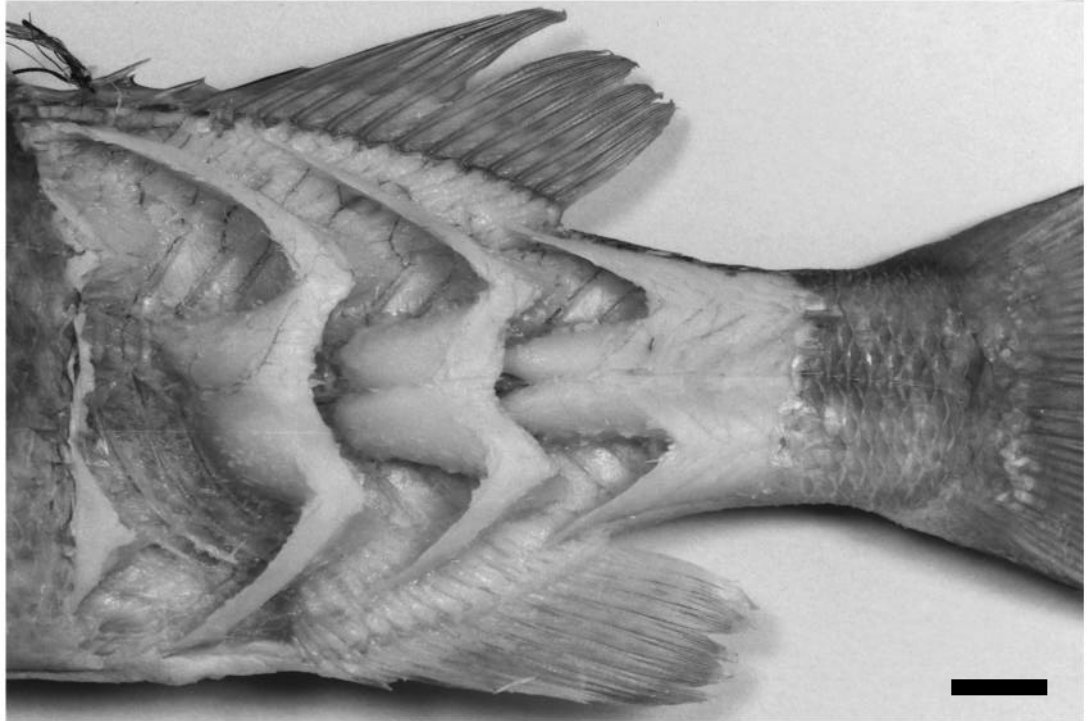
of the flow tank. At the conclusion of each experiment, fish were killed with an overdose of anesthetic and fixed in formalin to allow *post-mortem* dissections and X-rays.
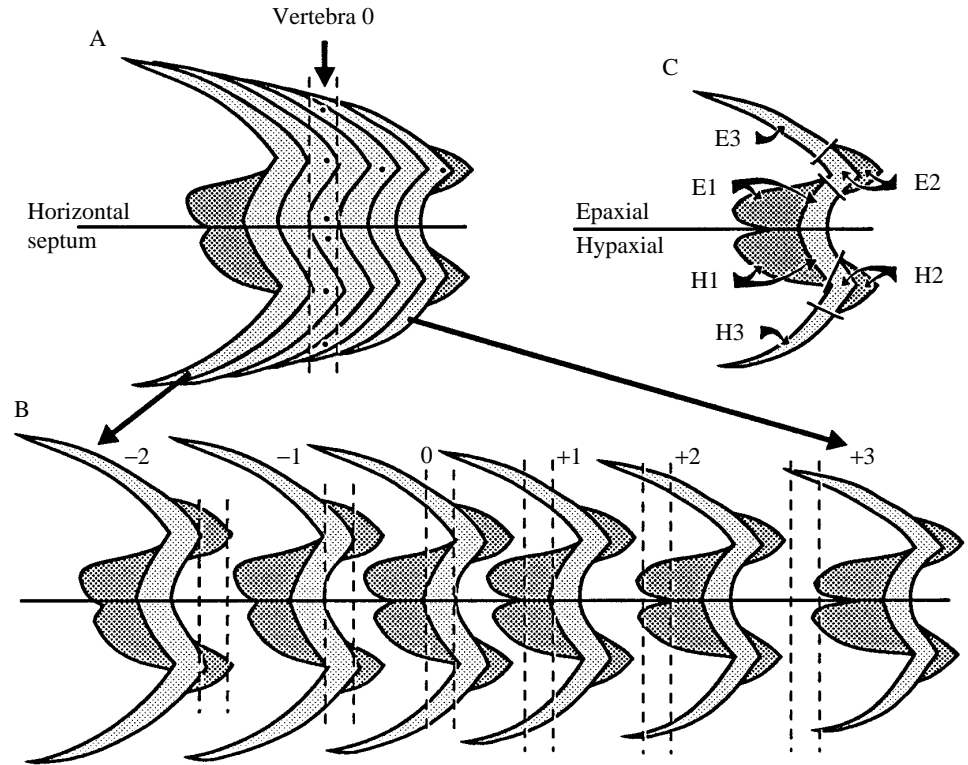
Electromyography

After anesthetizing the fish (with a 0.06 % solution of buffered tricaine methanesulphonate), we implanted eight bipolar electrodes in both the right and left sides of the fish using the pattern shown in Fig. 2A. During electrode implantation, anesthesia was maintained with a 0.03 % solution of anesthetic and water was passed over the gills with a peristaltic pump every 10–15 min. Approximately 0.6 mm of insulation was scraped off the recording ends of each wire of the bipolar electrode, and the general methods of electrode construction followed those of Jayne (1988). On each side of the fish, we attempted to implant six electrodes in a vertical row with a range in longitudinal position of less than the length of a single vertebra (Fig. 2A). This vertical row of six electrodes was located at approximately the same longitudinal position as the first spine of the anal fin (Fig. 1). As shown in Fig. 2B, for a given longitudinal location, by varying either the dorsal–ventral position or the depth of an electrode, it might be located in any one of six different myomeres. Two additional electrodes were implanted posterior to the vertical row (Fig. 2A) and were spaced approximately two vertebrae apart. These electrodes, together with one of the electrodes in the vertical row, formed a horizontal row of three electrodes. Sixteen electrodes were thus implanted into each fish. We generally attempted to implant all electrodes at a depth approximating half the distance between the skin and the midsaggital plane (Fig. 3), but we relied on *post-mortem* dissection to confirm the exact location of an electrode.

For each fish, we used the following criteria to select the electrodes for which EMGs were quantified and analyzed statistically. (1) Electrodes had to remain within the fish for the entire course of the experiment and during the process of fixation, so that we could use *post-mortem* X-rays and dissections to verify anatomical location. (2) The bare wire portion of both barbs of a single bipolar electrode had to lie clearly within the contractile tissue of a single myomere, as revealed by *post-mortem* dissection. (3) All 'vertical row' electrodes within an individual could not differ in longitudinal position by more than the length of one underlying vertebra, as revealed by *post-mortem* X-rays. (4) EMGs had to have sufficient amplitude to enable onset times to be reliably quantified. (5) The fibers in the region of the electrode could not show any conspicuous activity during slower steady swimming. In this way, we attempted to exclude electrodes from regions known to contain aerobic fibers for which the times of activation can differ significantly from those of deeper white myomeric muscle (Jayne and Lauder, 1994b). (6) We only used results from electrodes for which we could obtain ten quantifiable EMGs. (7) Finally, results were only analyzed from the side of each individual that had the most electrodes conforming to the above criteria.

Electromyograms (EMGs) were amplified $20\,000\times$ using Grass model P511 K preamplifiers with high and low bandpass filter settings of 100 Hz and 3 kHz, respectively, and a 60 Hz notch filter. The analog EMGs were recorded with a TEAC XR-7000 FM data recorder using a tape speed of 9.5 cm s^{-1}. A pulse generator provided coded output to both the NAC video system and the TEAC tape recorder, and allowed synchronization of EMGs and video records. We converted the analog signal to a digital file using a sampling rate of 8 kHz

Fig. 2. Semi-schematic left lateral view of the myomeres of *Micropterus salmoides* in the region of electrode implantation (anterior is to the left). The areas with light shading are the most superficial surfaces of the myomeres which are visible after removing only the skin. Regions with darker shading indicate medially projecting parts of the myomere that overlap longitudinally with adjacent myomeric muscle segments. (A) The approximate superficial pattern of EMG electrode implantation is indicated by the black dots. Six electrodes were placed in a vertical row and two additional electrodes were placed in the epaxial muscle approximately two and four vertebrae posterior to the vertical row of electrodes. Note that the actual myomere in which the electrode is located is highly dependent on the depth of the electrode. (B) An exploded view of the myomeres shown in A with the vertical dashed lines indicating the location of a single underlying reference vertebra. Note that, by aligning the myomeres by the dashed vertical lines, the normal myomeric relationships shown in A can be reconstructed. (C) Labeling conventions for electrode locations: E and H represent epaxial and hypaxial myomeric portions, respectively, and increasing numbers indicate greater distance away from the horizontal septum.

(Jayne *et al.* 1990). Because the rapid movements associated with unsteady swimming often resulted in a number of low-frequency artifacts, we filtered the digital EMGs using a finite impulse response filter that reduced the portion of the signal below 200 Hz to less than 10 % of its original amplitude.

To analyze the digitally filtered data, we used a custom-made computer program to determine the onset and offset time of muscle activity. Each EMG burst was displayed on a 15 inch VGA computer monitor such that 125 ms of data occupied the entire width of the monitor. An on-screen movable cursor was used to mark the times of onset and offset, and the resulting measurements were rounded to the nearest 0.1 ms. For one fish, both investigators independently digitized the onset and offsets

for each of the data channels, and we found that there was no significant difference in the data attributable to the individual who had made the measurements. Furthermore, the rank order of onset times of muscle activity was the same for both

Fig. 3. Transverse section showing the depth of the electrode sites used for statistical analysis (Table 1). Filled circles indicate sites within the vertical row of electrodes (see Fig. 2), whereas open circles indicate the two most posterior sites of the horizontal row. Note that the location of sites is only an approximation, in part because the symbols were positioned to avoid overlap. The diameter of the symbols closely approximates twice the length of the stripped wire at the recording end of the electrode. The illustration is based on a section near that of the vertical row (between the first and second caudal vertebrae) in a *Micropterus salmoides* with a total length of 25 cm. The stippled areas indicate the medial structures associated with the dorsal and anal fins (including musculature) as well as the vertebral centrum and neural and hemal arches. Superficial red muscle is indicated by the black triangular region near the horizontal septum.
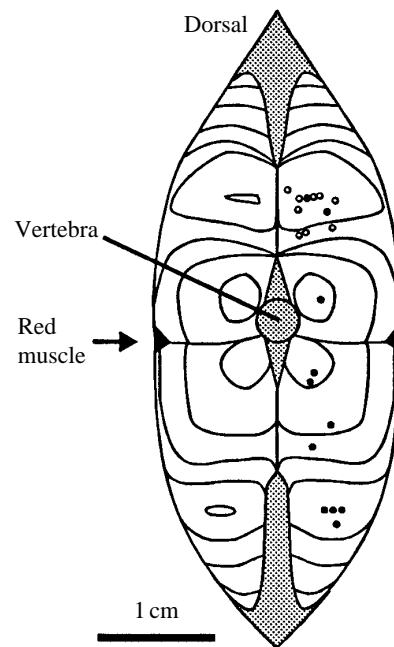
investigators. A single investigator determined the time of onset and offset for the remaining four fish.

Results

Morphology

In lateral view, the superficial portions of a myomere within *M. salmoides* resemble a W-shaped structure with its top oriented anteriorly and centered on the horizontal septum (Figs 1, 2). At the base of the W shape, two cones project postero-medially, whereas the portions of the myomere closest to the horizontal septum project antero-medially to form additional cone-like structures. Because of the convoluted shape of myomeres, at a longitudinal location spanning the length of only a single vertebra, contractile tissue may be present from as many as six different myomeres (Fig. 2).

For the sake of convenience, we will refer to the different 'portions' of the myomere using the letters E and H to indicate epaxial and hypaxial portions, respectively. Numbers following the letters designate the distance of the myomeric fibers from the horizontal septum. Thus, regions E3 and H3 indicate the extreme dorsal and ventral portions of the myomere, where the myosepta are nearly perpendicular to the midsaggital plane; in a lateral view, the deeper portions of the myomere in the region are not generally visible because they are directly medial to the superficial surface of the myomere (Fig. 2B,C). In contrast, the deep portions of the myomere nearest the horizontal septum (E1 and H1) project anteriorly from the superficial surface of the myomere for a distance of slightly more than two vertebrae (Fig. 2B,C). The remaining regions of the myomeres have deep portions that project posteriorly from the superficial surface for a distance slightly more than one vertebra (Fig. 2B,C). Although this scheme of designating portions of the myomere is useful for describing electrode locations on the basis of gross anatomical landmarks, it is important to emphasize that such designations may have little relationship to the finer details of myomeric anatomy. In addition, we numbered myomeres relative to the position of the vertical row: myomere 0 is the myomere whose central lateral portion is opposite vertebra 0 (Fig. 2). The abbreviation MY–2H3 refers to the H3 portion of the myomere two myotomes anterior (hence the –2) to myotome 0.

Some longitudinal variation in morphology was apparent in the myomeres from which we obtained EMGs (Fig. 2A,B). For example, within each individual, the most anterior myomere containing an electrode was always the largest myomere, and overall myomere size decreased posteriorly (Fig. 2B). The symmetry of the myomeric shape about the horizontal septum increased posteriorly, and this was particularly noticeable for the E1 and H1 regions of the myomere (Fig. 2B, MY–2 *versus* MY3). The anterior portions of the most anterior myomere implanted in these experiments were often opposite the most posterior trunk vertebra, whereas the entire longitudinal extent of myomeres posterior to myomere 0 was limited entirely to the region of the caudal vertebrae.

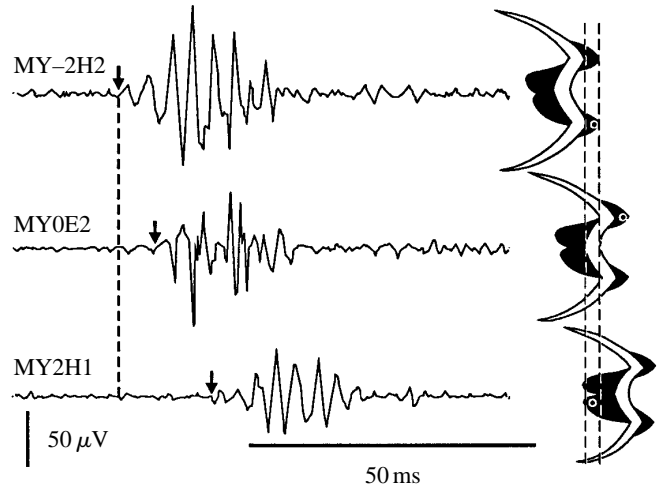Hereafter, we will use the term 'longitudinal position' to

Fig. 4. Electromyograms recorded simultaneously from three different locations on the same side within a single individual. Approximate electrode location is shown as the dot in the myomeres to the right of each EMG, and arrows indicate EMG burst onset times. Note that EMGs from more posterior myomeres have later onset times. For example, the electrodes in the myomere two myomeres anterior to vertebra 0 (MY–2H2) is active approximately 10 ms *prior* to the electrode in the myomere two myomeres posterior to vertebra 0 (MY2H1), even though both electrodes are at the same longitudinal position (as indicated by the fact that both dots are within the vertical dashed lines).

indicate electrode location as an anterior–posterior distance (expressed in numbers of vertebrae), irrespective of the myomere containing an electrode. In contrast, 'myomeric position' will indicate electrode location based on counting myomeres from anterior to posterior along the superficial portion of the horizontal septum.

Electromyography

Within individual fish, paired *t*-tests commonly revealed significant ($P<0.05$) differences in the timing of activity between pairs of ipsilateral electrodes. Three important findings are illustrated in Fig. 4. First, for electrodes with the same longitudinal position (Fig. 4, MY–2H2 and MY2H1), the onset of activity in the more posterior myomeric position (MY2H1) lagged behind that of the more anterior myomeric position (MY–2H2). Second, for electrodes with different longitudinal positions (Fig. 4, MY0E2 and MY2H1), the electrode with the more posterior longitudinal position (MY0E2) may have EMG onset times significantly *before* those from a more anterior longitudinal position when the latter site (MY2H1) has the more posterior myomeric position. Consequently, muscle activity was propagated posteriorly on the basis of myomeric position. Third, the durations of the EMGs from different sites were effectively identical.

The relative importance of myomeric *versus* longitudinal position is further illustrated for the combined data from all five individuals (Fig. 5). To allow onset times to be pooled for different individuals, values were converted to times that were relative to the mean values of all sites within each individual,
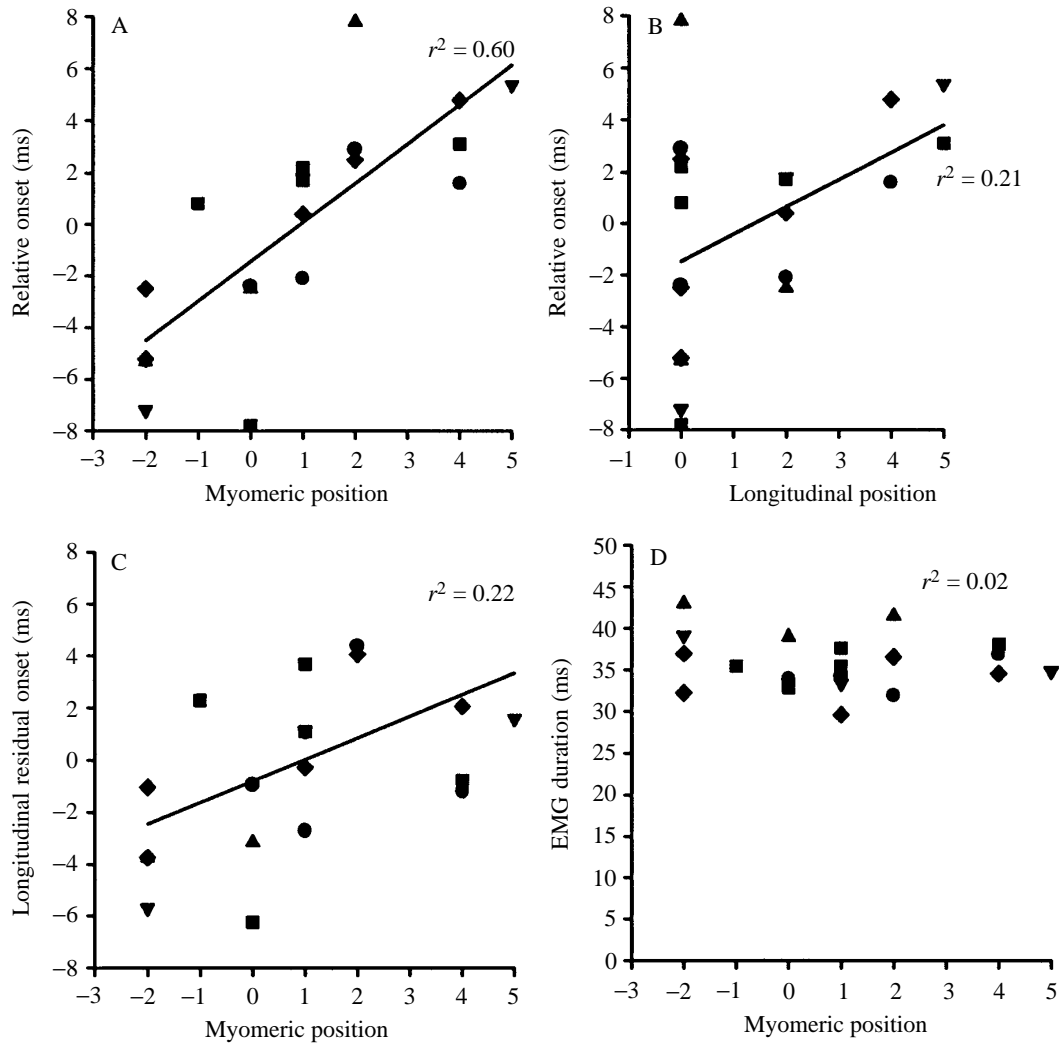
Fig. 5. Mean values of EMG variables for each recording site within each of five different individuals (indicated by different symbols). (A) The relative times of EMG onset *versus* myomeric position (see Fig. 2B) are significantly correlated. (B) The relative onset times show a marginally significant correlation with longitudinal position, but note that for vertebra 0, opposite the vertical row, the variance in onset times is extremely high. (C). Residual onset times are the difference between observed values and those predicted from a regression of onset time *versus* longitudinal position. (D) EMG duration was not significantly correlated with myomeric position. Note that myomeric position is based on counting myomeres from anterior to posterior, whereas longitudinal position is based on counting numbers of vertebrae from anterior to posterior.

and these relative times of EMG onset are shown in Fig. 5A. For the combined data, the relative onset times of muscle activity (in ms) showed a highly significant linear relationship to myomeric position (Fig. 5A, $P<0.0001$, regression slope=1.52, intercept=-1.44 ms), whereas these onset times had a only a marginally significant linear relationship with longitudinal position (Fig. 5B, $P=0.04$, regression slope=1.06; intercept=-1.49 ms). Furthermore, the large variance in the relative onset times at vertebra 0 (the location of the vertical row) compared with that at other longitudinal positions (Fig. 5B) probably results from the highly variable myomeric position of electrodes at this region.

When the longitudinal spacing between electrodes is minimal, there is little correlation between longitudinal position and myomeric position, but as the longitudinal distance between sites increases, a correlation does exist. For

example, the electrodes opposite vertebrae 4 and 5 invariably had the highest values of myomeric position (Table 1). Thus, to account for the potentially confounding effects of these intercorrelated variables, we further analyzed the relationships between onset times and electrode locations both for all data combined and for the large subset of sites from a more restricted longitudinal spacing (electrodes opposite vertebrae 0 and 2).

Fig. 5C shows the residual values of relative onset time obtained by taking the difference between each observed relative onset time and the value predicted from the regression based on the longitudinal position of the electrode (Fig. 5B). For the combined data (vertebrae 0–5), these residual values (Fig. 5C) had only a marginally significant ($P=0.036$) positive correlation with myomere position, whereas for data restricted to the two most anterior longitudinal positions, this correlation

was clearly significant ($P=0.003$). Thus, a significant amount of variance in the relative onset times was not accounted for by using only longitudinal position to designate electrode location.

A multiple regression predicting relative onset time from both myomeric and longitudinal positions (using all the data in Fig. 5A, $N=20$) was highly significant ($r^2=0.66$; $P=0.0001$). The regression coefficient for myomeric position (2.11) was highly significant ($P=0.0001$), whereas the coefficient for longitudinal position (-0.90) was not significant ($P=0.11$), and the intercept (0.75 ms) did not differ significantly ($P=0.34$) from zero. Consequently, our observations of the relative onset times among different locations in the deep myomeric musculature showed that, after accounting for electrode location by using myomeric position, longitudinal position had no significant predictive value for the timing of muscle activity.

The regression coefficients for myomeric position in the various models predicting relative onset time ranged from approximately 1.5 to 2.1, and these values conveniently estimate the intersegmental lag times (in ms segment^{-1}) for our observations of the burst-and-glide swimming of *M. salmoides*. In view of these very small values of intersegmental lag time, one might expect that the heterogeneity of activity at a single longitudinal position could be easily overlooked without considerable replication and very precise determination of onset times.

The duration of muscle activity from the deep regions of the myomere showed no significant ($P=0.60$) correlation with either myomeric position (Fig. 5D) or longitudinal position ($r^2=0.002$; $P=0.84$). The grand mean for the EMG durations from these deep myomeric sites (using data in Fig. 5D) was 35.8 ms ($N=20$, S.D.$=3.3$ ms).

EMG durations differed only slightly (one-way ANOVA, $P=0.01$) among the five individuals used in our experiments, and Tukey *post-hoc* comparisons of means revealed that only individual 3 differed from both individuals 1 and 5 (Table 1). Consequently, substantial differences in locomotor speed appeared unlikely to be confounding our analysis. Because of the lack of either rhythmic movements or the rhythmic occurrence of EMGs during burst-and-glide swimming, no simple methods were available to standardize EMG durations and relative onset times to a percentage of the cycle duration. However, when we performed alternative regression analyses after standardizing relative onset times to a percentage of the mean EMG duration for each individual, no conclusions differed from analyses using values expressed in milliseconds. Furthermore, the greatest change in the value of r^2 in any recalculated regression was only 0.02.

Previous experiments (Jayne and Lauder, 1994*b*) with a closely related species of centrarchid fish (*Lepomis macrochirus*) have found significant differences in the onset and duration of EMGs (expressed in ms) for the deep white myomeric musculature compared with those of the superficial red muscle near the horizontal septum. Hence, we deliberately excluded some data from sites in the present study showing

Table 1. *Mean values of EMG onset times and durations*

Individual	Myomeric portion	Myomeric position (myomeres)	Longitudinal position (vertebrae)	Onset (ms)	Duration (ms)
		Electrode location			
1	H1	0	0	-2.4 ± 3.5	33.8 ± 5.4
1	E2	1	2	-2.1 ± 2.1	34.2 ± 5.5
1	E1	2	0	2.9 ± 3.0	31.9 ± 6.8
1	E2	4	4	1.6 ± 2.1	36.8 ± 8.0
2	E2	-1	0	0.8 ± 1.9	35.4 ± 7.2
2	H2	0	0	-7.8 ± 2.3	32.8 ± 7.0
2	E2	1	2	1.7 ± 2.0	37.5 ± 6.6
2	H1	1	0	2.2 ± 1.8	35.4 ± 6.8
2	E2	4	5	3.1 ± 2.5	38.0 ± 7.2
3	H2	-2	0	-5.3 ± 3.2	42.9 ± 5.0
3	E2	0	2	-2.5 ± 2.0	38.9 ± 10.8
3	H1	2	0	7.8 ± 2.5	41.4 ± 6.5
4	H2	-2	0	-7.2 ± 3.0	39.1 ± 12.6
4	E2	1	2	1.8 ± 2.5	33.3 ± 6.2
4	E2	5	5	5.4 ± 2.4	34.8 ± 8.1
5	E2	-2	0	-2.5 ± 2.1	32.2 ± 3.7
5	H2	-2	0	-5.2 ± 2.0	36.9 ± 3.7
5	E2	1	2	0.4 ± 1.8	29.6 ± 3.3
5	H1	2	0	2.5 ± 1.9	36.5 ± 3.7
5	E2	4	4	4.8 ± 1.8	34.5 ± 4.4

Conventions for designating the electrode location are given in Fig. 2C.

Timing variables are given as mean ± S.D., $N=10$.

activity during steady swimming near sustainable speeds or other traits characteristic of red muscle. Fig. 6 illustrates some of these data (MY–2E2) excluded from our primary analysis. For a pair of electrodes within the same myomere of a single fish during relatively fast semi-steady swimming that lacked the kinematics characteristic of the burst-and-glide mode, one site (MY–2E2) showed substantial muscle activity whereas the other site lacked any noticeable activity during this type of behavior (Fig. 6A). In contrast, during faster burst-and-glide swimming, both sites had detectable muscle activity (Fig. 6B), although one site (MY–2E2) had an earlier onset time and longer duration than those of the other site. These observations for *M. salmoides* closely parallel those observed previously for *L. macrochirus*. However, the site in *M. salmoides* (Fig. 6, MY–2E2) with activity similar to that of red muscle was not in the superficial strip of muscle located near the horizontal septum; instead, it was clearly in a location with a depth very similar to other epaxial sites (Fig. 3) that otherwise displayed a pattern more typical of the white myomeric musculature. These results suggest either that aerobic fibers are located in certain regions of deep myomeric cones of *M. salmoides* or, perhaps, that certain populations of deep anaerobic fibers have different thresholds for recruitment from those of other adjacent white fibers.

In our experiments with *M. salmoides*, we commonly observed a lack of detectable activity from regions E3 and H3

A

MY–2E2
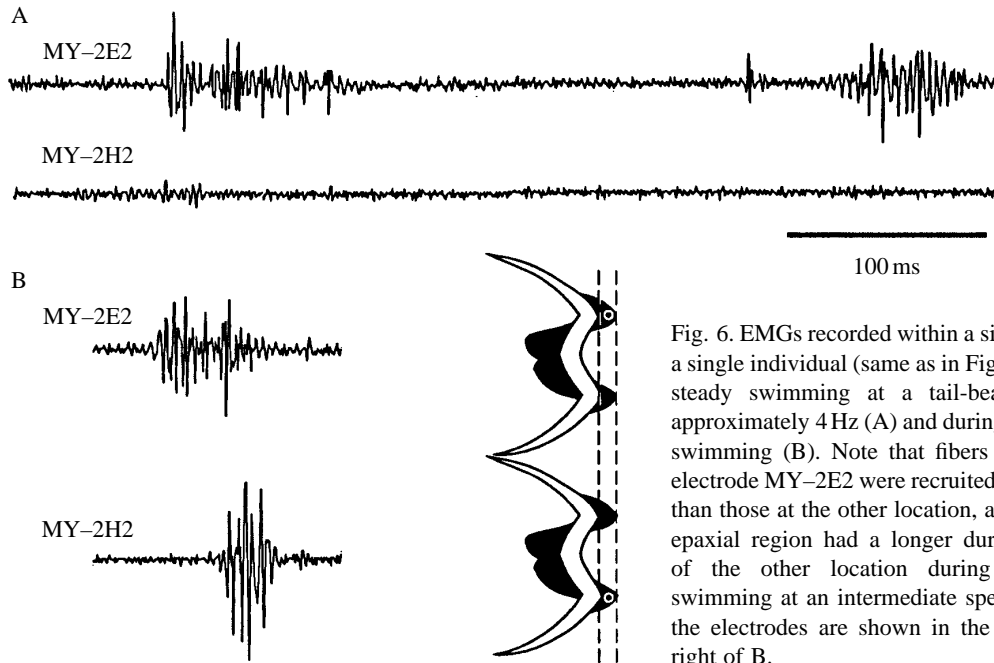
MY–2H2

100 ms

B

MY–2E2

MY–2H2

Fig. 6. EMGs recorded within a single myomere in a single individual (same as in Fig. 4) during semi-steady swimming at a tail-beat frequency of approximately 4 Hz (A) and during burst-and-glide swimming (B). Note that fibers recorded by the electrode MY–2E2 were recruited at slower speeds than those at the other location, and EMGs of this epaxial region had a longer duration than those of the other location during burst-and-glide swimming at an intermediate speed. Locations of the electrodes are shown in the diagrams to the right of B.

when EMGs from other myomeric regions were readily quantifiable (Table 1). Establishing an absence of muscle activity is complicated by the fact that such a finding could result from a variety of technical shortcomings, such as a bad electrode. However, some evidence from our experiments suggests that such an absence of observed activity in regions E3 and H3 reflects a real biological phenomenon. For example, in one individual, we elicited an escape response (Fig. 7) and the EMGs from all regions including E3 and H3 were similar to those previously reported for this type of behavior (Jayne and Lauder, 1993). In addition, EMGs from regions H3 and E3 could occasionally be observed at times that were distinctly different from those of other electrodes in different portions of ipsilateral myomeres (Fig. 8). Fig. 9 shows EMGs from a different individual from the one that was used for the all other illustrations of EMGs, and it appears that regions 1 and 2 of the myomere are utilized more commonly than region 3. For the data shown in Fig. 9, regions E3 and H3 had detectable activity when other myomeric regions had EMGs with relatively short duration and high amplitude. Hence, as swimming movements become more vigorous, the probability of observing activity in regions E3 and H3 increased (Figs 7 and 9B).

Discussion

In summary, for burst-and-glide swimming of *M. salmoides*,

Fig. 7. EMGs recorded from the left (top five traces) and right sides (bottom two traces) during an escape response from the same individual for which data are shown in Fig. 5. Note that all portions of the myomere are simultaneously activated during the stage 1 EMG on the left side. This is similar to the pattern reported elsewhere for red and white muscle activity during C-starts in centrarchid fish (Jayne and Lauder, 1993).

muscle activity is propagated posteriorly, with EMGs of posterior myomeres lagging behind those of more anterior

MY1E3

MY0E2

MY2H1

MY–2H2

MY–1H3

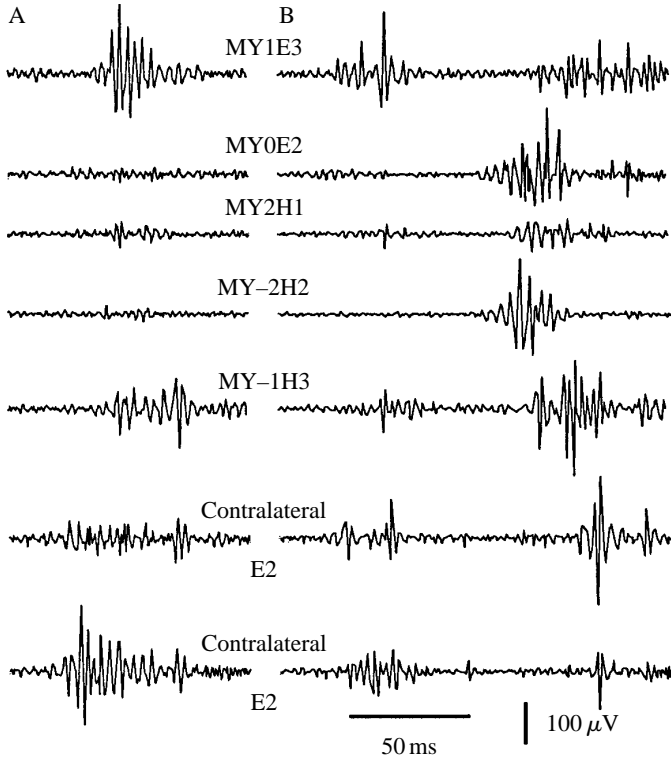Contralateral E2

Contralateral E2

250 μV

50 ms
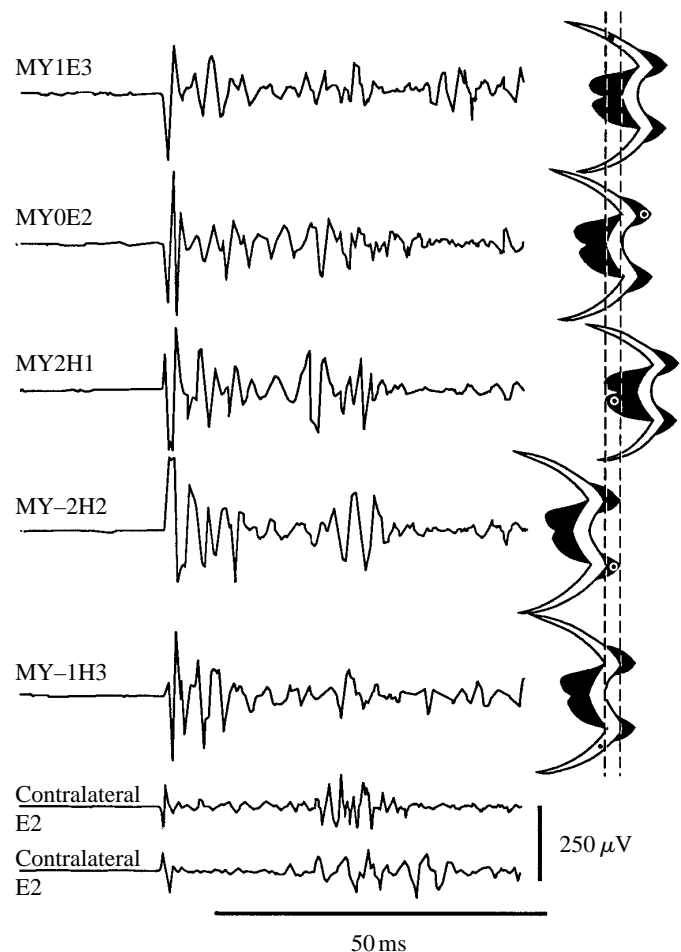
Fig. 8. Burst-and-glide swimming EMGs recorded from the same individual and electrode sites as shown in Fig. 7. Note that the intensity of recruitment of fibers in the extreme dorsal (E3) and ventral (H3) portions of the myomere may vary independently of the recruitment of fibers in ipsilateral sites that are closer to the horizontal septum. (A) Slower-speed swimming; (B) faster-speed swimming.
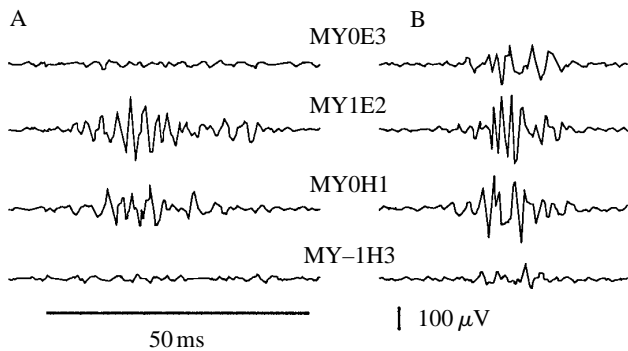

Fig. 9. Burst-and-glide swimming EMGs recorded from four sites within the vertical row of electrodes from a different individual from that used for all other illustrations of muscle activity. Note that A (slower-speed swimming) was recorded before the data shown in B (faster-speed swimming); hence, the lack of activity in the E3 and H3 regions of the myomere cannot be attributed simply to damaged recording sites in these regions.

myomeres regardless of the longitudinal position relative to the vertebral column. Furthermore, for this mode of unsteady swimming, large portions (E1, E2, H1 and H2) of each myomere have synchronous times of onset and equal durations

of activity. Thus, the central fibers of each myomere appear to be active synchronously.

The technical difficulties in obtaining these data were considerable. Because of the unsteady nature of the burst-and-glide mode of swimming in *M. salmoides*, the speed of swimming could not be easily controlled, and the speed with which the fish undulates determines whether or not white muscle will be recruited. As the speed of locomotion increases for axial motor patterns that involve a posterior propagation of activity, the intersegmental lag times decrease (Grillner and Kashin, 1976; Jayne and Lauder, 1994*b*). Hence, we faced tradeoffs between trying to make the fish swim fast enough so that deep myomeric muscle had EMGs with amplitudes sufficiently high to quantify the signal and at the same time having the fish swimming slowly enough for there to be substantial intersegmental lag times which would facilitate detection of heterogeneous activity among the myomeres at a single longitudinal location. An additional drawback of having minimal control over the speed and direction of the swimming fish was that very often the position of the fish in the flow tank caused the electrode wires to rub against the sides of the tank. Data from such events were identified using the simultaneous dorsal and lateral video recordings, but such events were frequent during bouts of burst-and-glide swimming. At higher swimming speeds, we also discarded numerous sequences where vibrations of the main electrode cable appeared to be generating artifacts. Hence, of necessity, we were very selective in the sequences that we analysed.

Detailed descriptions of the muscular and neural anatomy of *M. salmoides* are lacking; however, within a sample of centrarchid fish including *M. salmoides*, the shape of complete myomeres is known to vary considerably both longitudinally within a single individual and among different species (Jayne and Lauder, 1994*a*). Furthermore, the longitudinal span of myomeres may also vary both longitudinally and among different species when values are expressed in either absolute distances or numbers of underlying vertebrae (Westneat *et al.* 1993; Jayne and Lauder, 1994*a*). In the caudal region of *M. salmoides*, six different myomeres may be found opposite a single vertebra, and intersegmental lag times approximated 1.7 ms. Thus, timing differences of up to approximately 10 ms would be expected among different myomeres at a single longitudinal location in *M. salmoides*. For species with a greater longitudinal overlap of myomeres than that of *M. salmoides*, it seems likely that even greater heterogeneity of timing could be found among the deep myomeric fibers within a given cross section of the fish.

The most detailed descriptions of neuroanatomy relevant to myomere function are those of Westerfield *et al.* (1986) for the zebrafish *Brachydanio rerio*. In zebrafish, within each spinal segment there are three distinct primary motoneurons and, on the basis of the locations of the cell bodies in the rostral, middle and caudal regions within a spinal segment, these motoneurons are designated RoP, MiP and CaP, respectively. In the trunk region of the zebrafish, the territories of the myomere innervated by the primary motoneurons do not overlap. Using

the nomenclature for myomeric regions shown in Fig. 2C, the territory of MiP corresponds roughly to that of E1, the territory of RoP is the dorsal portion of H1, and CaP innervates the region of H1 that is ventral to the territory of RoP. There are several more secondary motoneurons per spinal segment than the number of primary motoneurons and, unlike the primary neurons, the secondary motoneurons may innervate muscle fibers from more than one myomere. For the zebrafish, Westerfield *et al.* (1986) did not describe the innervation of the extreme dorsal (E3) and ventral (H3) portions of the myomere. On the basis of the available illustrations, it appears that the longitudinal extent of the myomeres in zebrafish may be two or three vertebrae fewer than that of *M. salmoides*.

Liu and Westerfield (1988) suggested that high- and low-amplitude EMG spikes recorded from myomeric muscle were correlated to output from the primary and secondary motoneurons, respectively and, on the basis of the amplitudes the EMG spikes of swimming zebrafish, they concluded that the primary motoneurons of a single segment were usually, but not always, co-activated. The EMGs that we recorded from *M. salmoides* did not show any conspicuous bimodal distribution of spike amplitudes (Figs 4, 6–9); however, as discussed previously, we did analyze results from a restricted range of swimming speeds. Consequently, it is not altogether clear how our recordings of muscle activity might correspond to the scheme of recruitment proposed by Liu and Westerfield (1988). However, it is intriguing that the regions (E1, E2, H1 and H2) within the myomeres that we found to be co-activated in *M. salmoides* do correspond closely to the portions of zebrafish myomeres that are innervated collectively by the primary motoneurons.

We did encounter some unexpected complexity in the patterns of muscle activity within the myomeres of *M. salmoides*. For example, it appears that, during burst-and-glide swimming, the activity of the E3 and H3 region can be decoupled from that of regions of the myomere that are closer to the horizontal septum. Furthermore, some fibers which were fairly deep and nearly 1 cm away from the horizontal septum showed activity similar to that described for the pocket of superficial red muscle close to the horizontal septum (Jayne and Lauder, 1994b). The large numbers of motoneurons innervating a single myomere would be expected to contribute to the potential for complex patterns of myomeric muscle activity, such as those we have observed in *M. salmoides*.

Rome and Sosnicki (1991) preserved carp in a laterally flexed position and then took samples from muscle fibers within a cross section in order to estimate the length changes of the sarcomeres from fibers of varying orientation distributed throughout the myomeric musculature. For ipsilateral samples of white fibers within a given cross section, Rome and Sosnicki (1991) found a remarkable uniformity in sarcomere length; hence, they concluded that different regions of the white myomeric muscle would have similar *in vivo* rates of shortening and production of force. Because our observations for *M. salmoides* showed that the onset times within a cross section could easily differ by 9 ms, there should be noticeable phase shifts between onsets of electrical activity and the length changes undergone by the fibers, despite the fact that fibers within a cross section have similar total strain. The times to peak tension and to half-relaxation for an isometric twitch of the white muscle of *M. salmoides* are approximately 11 and 21 ms, respectively (Johnson *et al.* 1994), while EMG durations generally exceed 30 ms. Consequently, fibers within a cross section of *M. salmoides* would generally have more than 20 ms of synchronous electrical activity, and there may be relatively minor mechanical effects resulting from the heterogeneity of onset times.

Although a large proportion of muscle fibers within a myomere appears to be activated as a unit, it is still not obvious what the fundamental functional units are during undulatory locomotion in the intact fish. Alexander (1969) suggested that the fibers of the deep myomeric musculature form epaxial and hypaxial helical trajectories that include the most dorsal and ventral regions of the fish, respectively, and that these trajectories include the fibers of several myomeres. Our observations of sequential activation of muscle based on myomeric position and the frequent absence of activity in regions E3 and H3 make it difficult to envision how such helical trajectories of muscle might function.

Westneat *et al.* (1993) suggested that the anteriorly projecting cones (regions E1 and H1) of scombrid fish myomeres function as a conic section whose length decreases as diameter increases during the activation of muscle, resulting in a pressure that stretches connective tissue. Because scombrids show numerous specializations in myomeric morphology and distribution of fiber type (Westneat *et al.* 1993), comparisons with other taxa must be regarded with caution. However, on the basis of our observations of *M. salmoides*, more than one myomere is nested within such a conic section and muscle appears to be activated sequentially by myomere. Thus, not all of the contractile tissue within such a conic section would be activated simultaneously and predicting shape and pressure changes may be more complicated than previously supposed.

With respect to general suggestions that myomeric activity generates pressure (Wainwright, 1983), it is also not clear what happens if the central portions of the myomere are activated while regions E3 and H3 are inactive. The myosepta are one of many connective tissue structures that could potentially constrain both changes in the shape of the myomere and the resultant pressure changes, but the importance of the myosepta relative to other connective tissue is not clear. As lamented by Wainwright (1983), we lack the direct observations of myomeric shape change that are critically important for the hypotheses that suggest the production of pressure is a significant means of producing or transmitting locomotor forces.

Our observations of myomeric muscle activity in *M. salmoides* emphasize the utility of using electromyography to determine experimentally *in vivo* patterns of muscle use. In the case of the myomeres of fish, both the gross morphology and the neuroanatomy are sufficiently complex to allow an almost limitless number of possible mechanisms to be proposed for

the neural control and mechanical function of these structures. However, we found that much of the variance in the times of deep myomeric muscle activity was explained quite simply by the posterior propagation of muscle activity based on the sequential activation of myomeres rather than longitudinal position based on the location of vertebral segments. We also encountered some unexpected diversity of muscle activity, especially in extreme dorsal and ventral myomeric fibers, which suggests a lack of obligatorily simultaneous activation of the entire myomere. Thus, clearer boundary conditions are now available for refining explanations of both the mechanical behavior of this system and its neural control.

References

ALEXANDER, R. McN. (1969). The orientation of muscle fibres in the myomeres of fishes. *J. mar. Biol. Ass. U.K.* **49**, 263–290.

BONE, Q. (1978). Locomotor muscle. In *Fish Physiology*, vol. VII, *Locomotion* (ed. W. S. Hoar and D. J. Randall), pp. 361–424. New York: Academic Press.

BONE, Q. (1989). Evolutionary patterns of axial muscle systems in some invertebrates and fish. *Am. Zool.* **29**, 5–18.

BONE, Q. AND ONO, R. D. (1982). Systematic implications of innervation patterns in teleost myotomes. *Breviora* **470**, 1–23.

FETCHO, J. R. (1986). The organization of the motoneurons innervating the axial musculature of vertebrates. I. Goldfish (*Carassius auratus*) and mudpuppies (*Necturus maculosus*). *J. comp. Neurol.* **249**, 521–550.

GREENE, C. W. AND GREENE, C. H. (1914). The skeletal musculature of the king salmon. *Bull. Bur. Fish.* **33**, 25–59.

GRILLNER, S. AND KASHIN, S. (1976). On the generation and performance of swimming in fish. In *Neural Control of Locomotion* (ed. R. M. Herman, S. Grillner, P. S. G. Stein and D. G. Stuart), pp. 181–201. New York: Plenum Press.

HUDSON, R. C. L. (1969). Polyneuronal innervation of the fast muscles of the marine teleost, *Cottus scorpius* L. *J. exp. Biol.* **50**, 47–67.

JAYNE, B. C. (1988). Muscular mechanisms of snake locomotion: An electromyographic study of lateral undulation of the Florida banded water snake (*Nerodia fasciata*) and the yellow rat snake (*Elaphe obsoleta*). *J. Morph.* **197**, 159–181.

JAYNE, B. C. AND LAUDER, G. V. (1993). Red and white muscle activity and kinematics of the escape response of the bluegill sunfish during swimming. *J. comp. Physiol.* A **173**, 495–508.

JAYNE, B. C. AND LAUDER, G. V. (1994a). Comparative morphology of the myomeres and axial skeleton in four genera of centrarchid fishes. *J. Morph.* **220**, 185–205.

JAYNE, B. C. AND LAUDER, G. V. (1994b). How swimming fish use slow and fast muscle fibers: implications for models of vertebrate muscle recruitment. *J. comp. Physiol.* A **175**, 123–131.

JAYNE, B. C., LAUDER, G. V., REILLY, S. M. AND WAINWRIGHT, P. C. (1990). The effect of sampling rate on the analysis of digital electromyograms from vertebrate muscle. *J. exp. Biol.* **154**, 557–565.

JOHNSON, T. P., SYME, D. A., JAYNE, B. C., LAUDER, G. V. AND BENNETT, A. F. (1994). Modeling red muscle power output during steady and unsteady swimming in largemouth bass. *Am. J. Physiol.* **267**, R481–R488.

LIU, D. W. AND WESTERFIELD, M. (1988). Function of identified motoneurones and co-ordination of primary and secondary motor systems during zebrafish swimming. *J. Physiol., Lond.* **403**, 73–89.

NURSALL, J. R. (1956). The lateral musculature and the swimming of fish. *Proc. zool. Soc., Lond.* **126**, 127–143.

ROME, L. C. AND SOSNICKI, A. A. (1991). Myofilament overlap in swimming carp. II. Sarcomere length changes during swimming. *Am. J. Physiol.* **260**, C289–C286.

WAINWRIGHT, S. A. (1983). To bend a fish. In *Fish Biomechanics* (ed. P. W. Webb and D. Weihs), pp. 68–91. New York: Praeger Publishers.

WESTERFIELD, M., McMURRAY, J. V. AND EISEN, J. S. (1986). Identified motoneurons and their innervation of axial muscles in the zebrafish. *J. Neurosci.* **6**, 2267–2277.

WESTNEAT, M. W., HOESE, W., PELL, C. A. AND WAINWRIGHT, S. A. (1993). The horizontal septum: Mechanisms of force transfer in locomotion of scombrid fishes (Scombridae, Perciformes). *J. Morph.* **217**, 183–204.